Structures and dynamic features of dinuclear tartratozirconocene complexes

Gerhard Erker*, Mathias Rump
Organisch-Chemisches Institut der Universität Münster, Corrensstrasse 40, D-4400 Münster (FRG)

Carl Krüger and Matthias Nolte
Max-Planck-Institut für Kohlenforschung, Kaiser-Wilhelm-Platz 1, D-4330 Mülheim an der Ruhr (FRG)

Abstract

The reaction of dimethylzirconocene with 2*R*,3*R*-diethyltartrate proceeds with evolution of two equivalents of methane and yields the chiral diethyltartratozirconocene dimer **2**. The analogous reaction between $Cp_2Zr(CH_3)_2$ and 2*S*,3*S*-diethyltartrate furnishes *ent*-**2** in almost quantitative yield. Complex **2** contains a dimetallatricyclic framework (tetraoxadizirconatricyclo[5.3.0.$0^{2,6}$]decane) in solution as well as in the solid state. Complex **2** was characterized by X-ray diffraction. It crystallizes in space group $P2_1$ with cell parameters $a = 9.494(1)$, $b = 20.122(2)$, $c = 9.915(1)$ Å, $\beta = 108.36(1)°$, $Z = 2$, $R = 0.039$ and $R_w = 0.046$. In solution the tartratozirconocene dimer **2** undergoes an intramolecular automerization reaction ($\Delta G^{\ddagger}_{intra}$ (265 K) $\approx 13 \pm 1$ kcal mol^{-1}) which probably proceeds via a ten-membered metallacyclic intermediate or transition state. A cross-over experiment between the enantiomeric complexes **2** and *ent*-**2** showed the activation barrier for intermolecular exchange of mononuclear dioxazirconacyclopentane units $Cp_2\overline{Zr}OCH(E)\overline{CH(E)}O$ ($E = CO_2C_2H_5$) leading to equilibration with the isomeric dinuclear tartratozirconocene complex *meso*-**2** to be at $\Delta G^{\ddagger}_{inter}$ (290 K) $\approx 22 \pm 1$ kcal mol^{-1}. Complex *meso*-**2** shows NMR spectra compatible with a static ten-membered dimetallamonocyclic ring structure. The reaction of dimethylzirconocene with *meso*-dimethyltartrate yields the (*meso*-dimethyltartrato)zirconocene dimer **4** (two isomers, **4a** and **4b** in a 60:40 ratio, both of which possess dynamic dimetallatricyclic structures in solution ($\Delta G^{\ddagger}_{intra}$ (224 K) $\approx 11 \pm 1$ kcal mol^{-1} (**4a**); $\Delta G^{\ddagger}_{intra}$ (285 K) $\approx 14 \pm 1$ kcal mol^{-1} (**4b**); $\Delta G^{\ddagger}_{inter}$ (300 K) $= 24.7 \pm 1.0$ kcal mol^{-1} (**4a** → **4b**). Crystallization from methylene chloride gives single crystals of the isomeric (*meso*-dimethyltartrato)zirconocene dimer **5a** which contains a monocyclic ten-membered ring structure. Complex **5a** crystallizes in space group $P2_1/c$ with cell parameters $a = 11.261(2)$, $b = 14.511(2)$, $c = 11.562(2)$ Å, $\beta = 117.81(1)°$; $Z = 2$, $R = 0.047$ and $R_w = 0.063$.

Introduction

Oxazirconacycloalkanes and related Group 4 metal containing heterocycles show interesting stereoelectronic features. Attaching one or two ring oxygen atoms to the electropositive d-block element in the first place leads to a substantial increase of the electrophilicity of the early transition metal. This is caused by the strong electron withdrawing inductive effect of the σ-chalcogen ligand. The electron deficiency at the metal center can then be diminished in two different ways, namely either by mesomeric stabilization (i.e. oxygen to metal π-donation) or by means of dimerization. The former effect is observed in many oxazirconacycles with ring sizes >7, exhibiting monomeric structures in the solid state showing short oxygen to zirconium distances and rather large bonding angles at oxygen (see Scheme 1) [1]. In contrast, the oxametallacycles with ring size $\leqslant 5$ have a large tendency for dimerization [2]. Interestingly, some of the metallatricyclic dimers thus formed may undergo a subsequent ring opening reaction of the central Zr_2O_2 four-membered heterocycle to pro-

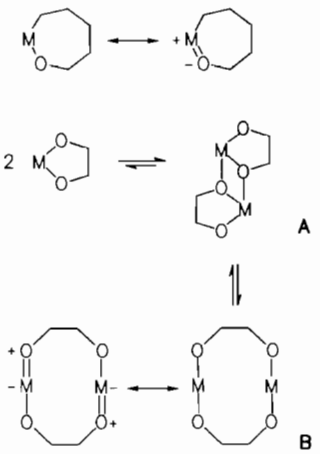

Scheme 1.

*Author to whom correspondence should be addressed.

0020-1693/92/$5.00

duce a medium-sized ring system containing two electrophilic metal centers [3]. In this situation, the Group 4 metal centers may now become electronically stabilized by the mesomeric effect of the adjacent oxygen atom, as mentioned above. This may result in the interesting situation that for some specific oxa–Group 4-metallacycloalkane systems both types of structures, the dimetallatricyclic type (**A**) and the isomeric dimetallamonocycle (**B**, see Scheme 1) are getting very close in energy. We have found several examples [4] where such a structural dichotomy can be observed experimentally. Here we wish to describe a typical set of such examples originating from the chemistry of tartratozirconocene complexes, where the favored molecular structure (e.g. dimetallatetraoxatricyclo[5.3.0.$0^{2,6}$]decane type (**A**) or ten-membered monocyclic ring system (**B**)) is very much dependent on both the specific stereochemical substitution pattern at the ring perimeter and additional external parameters (i.e. structural differences may be observed in solution and in the solid state).

Results and discussion

Reaction of dimethylzirconocene with 2R,3R- and 2S,3S-diethyltartrate

The tartratozirconocene complexes for this study were all prepared by reacting dimethylzirconocene with the respective dialkyltartrate in a 1:1 stoichiometry. We have thus treated $Cp_2Zr(CH_3)_2$ (**1**) with one molar equivalent of the 2*R*,3*R*-diethyltartrate enantiomer in methylene chloride solution at ambient temperature. Methane is evolved. The reaction proceeds very cleanly and gives an almost quantitative yield of the 3*R*,4*R*-configurated tartratozirconocene complex **2** (Scheme 2). Similarly, the reaction of dimethylzirconocene with 2*S*,3*S*-diethyltartrate furnished the 3*S*,4*S*-configurated tartratozirconocene enantiomer *ent*-**2**.

The optically active metallocene complex **2** is characterized by an optical rotation of $[\alpha]_D^{25} = +36.2°$ ($c = 10$ mg/ml, in CH_2Cl_2). In the solid state (KBr) it exhibits two strong CO stretching bands in the IR spectrum at $\nu(C{=}O) = 1748$ and 1711 cm^{-1}. Recrystallization from toluene gave single crystals of the zirconocene complex **2** which were suitable for an X-ray crystal structure analysis.

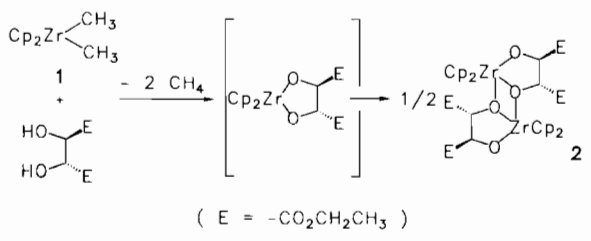

Scheme 2.

In the solid state the tartratozirconocene complex **2** is dimeric and contains a dimetallatricyclic framework. Two five-membered ZrOCCO ring systems are connected by means of a central Zr_2O_2 four-membered heterocycle. The three annulated metallacycles do not deviate much from planarity. The sums of bonding angles of the five-membered ring systems are 535.1 and 534.3°, respectively. The central dioxadizirconacycle is only slightly puckered (the sum of bonding angles within the ring is 355.4°).

There are two three-coordinate oxonium-type oxygen centers (the sums of bonding angles at O1 and O7 are 358.8 and 358.9°, respectively). The bonding angles inside the central Zr_2O_2 unit are large at the oxonium oxygens (Zr1–O1–Zr2: 113.7(2)°; Zr1–O7–Zr2: 113.9(2)° and small at zirconium (O1–Zr1–O7: 63.8(1)°; O1–Zr2–O7: 64.0(1)°). The zirconium–oxygen bonds within the central four-membered ring are nearly equidistant at 2.246(4) (O1–Zr1), 2.239(4) (O1–Zr2), 2.235(4) (O7–Zr2) and 2.243(3) (O7–Zr1) Å. The metal–oxygen separation between Zr and the adjacent two-coordinate oxygen centers is much smaller at 2.037(4) (O6–Zr1) and 2.043(4) (O12–Zr2) Å. The σ-ligand angle at zirconium (O1–Zr2–O12: 135.5(2)°; O6–Zr1–O7: 134.3(1)°) is large. There is a marked difference between the carbon–oxygen bond lengths at the three- and two-coordinate oxygen centers (1.413(7) (O1–C1) versus 1.367(7) (O6–C6) Å and 1.423(7) (O7–C21) versus 1.390(8) (O12–C26) Å, respectively). The ester substituents are attached to the carbon atoms C1, C6, C21 and C26 (which are all *R*-configurated). They are oriented alternatingly above and below the mean central framework to create a chiral near to C_2-symmetric overall molecular geometry of the dimetallatricyclic tartratozirconocene dimer **2** in the solid state.

A view of the molecular geometry of the dimetallatricyclic structure of the chiral diethyltartratozirconocene dimer **2** in the crystal with numbering scheme is given in Fig. 1. Selected bond lengths (Å) and angles (°) of **2** are listed in Table 1, and atomic coordinates in Table 2.

In solution complex **2** has an analogous dimeric C_2-symmetric structure. This is evident from the appearance of its ^1H NMR spectrum at low temperature. At 225 K in CD_2Cl_2 solution the ^1H NMR spectrum of **2** (200 MHz) shows the signals of two different $-CO_2CH_2CH_3$ substituents in a 1:1 intensity ratio (methyl triplets at δ 1.20 and 1.44; methylene multiplets at δ 4.30 and 4.07, respectively). The AX pattern of the –*CH*E–*CH*E–methine hydrogens of the symmetry-equivalent five-membered metallacyclic ZrOCH(E)–CH(E)O subunits (E = $-CO_2C_2H_5$) appears at δ 4.78 and 4.06 with a coupling constant of $^3J = 9.4$ Hz. The ^1H NMR resonances of the four cyclopentadienyl rings of the

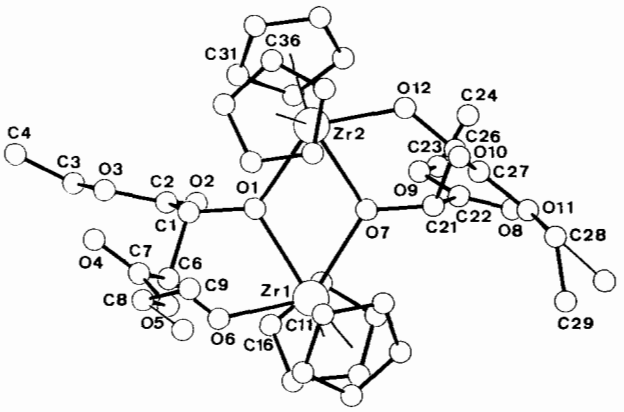

Fig. 1. A view of the molecular geometry of the dimetallatricyclic structure of the chiral diethyltartratozirconocene dimer **2** in the crystal with (crystallographic) numbering scheme (three ester methyl groups are disordered).

TABLE 1. Selected bond distances (Å) and angles (°) of **2**

Zr1–O1	2.246(4)	Zr1–O6	2.037(4)
Zr1–O7	2.243(3)	Zr2–O1	2.239(4)
Zr2–O7	2.235(4)	Zr2–O12	2.043(4)
O1–C1	1.413(7)	O6–C6	1.367(7)
O7–C21	1.423(7)	O12–C26	1.390(8)
C1–C6	1.562(9)	C21–C26	1.553(9)
O7–Zr1–O6	134.3(1)	O7–Zr1–O1	63.8(1)
O6–Zr1–O1	71.5(1)	O12–Zr2–O7	71.6(2)
O12–Zr2–O1	135.5(2)	O7–Zr2–O1	64.0(1)
C1–O1–Zr2	127.3(3)	C1–O1–Zr1	117.8(3)
Zr2–O1–Zr1	113.7(2)	C6–O6–Zr1	128.2(3)
C21–O7–Zr2	118.8(3)	Zr2–O7–Zr1	113.9(2)
C26–O12–Zr2	127.1(4)	C6–C1–O1	108.3(5)
C1–C6–O6	109.3(5)	C26–C21–O7	108.0(5)
C21–C26–O12	108.8(5)		

dimetallatricyclic diethyltartratozirconocene dimer **2** are isochronous and are observed at δ 6.24.

Complex **2** exhibits dynamic ^{1}H NMR spectra. With increasing temperature all of the above described ^{1}H NMR resonances except the Cp singlet are broadened and eventually pairwise coalescence of the –C*H*(E)–methine 'doublets' as well as the ester–ethyl resonances is observed. The limiting high temperature ^{1}H NMR spectrum (e.g. in C_6D_6, 200 MHz, 300 K) shows only one averaged set of signals of the $[Cp_2\overline{ZrOCH(E)CH(E)O}]_2$ species at δ 6.24 (s, 20H, Cp), 4.92 (s, 4H, –C*H*(E)), 4.08 (m, 8H, CH_2), and 1.06 (t, 12H, CH_3). From the coalescence of the methyl signals in CD_2Cl_2 solution we have estimated a Gibbs activation barrier of this equilibration process of $\Delta G^{\ddagger}$ (265 K) $\approx 13 \pm 1$ kcal mol^{-1} at the coalescence temperature. (The (tartrato)Ti(OR)$_2$ dimers employed in the catalytic 'Sharpless-epoxidation' of allylic alcohols show a similar dynamic NMR behavior [5].)

There are two possible pathways that could potentially lead to such an equilibration of –CH($CO_2CH_2CH_3$)–

TABLE 2. Atomic coordinates and isotropic thermal parameters (Å^2) of **2**

Atom	x	y	z	U_{eq}[a]
Zr1	0.0940(1)	0.0000	0.8622(1)	0.030(1)
Zr2	0.4540(1)	0.0222(1)	1.1558(1)	0.030(1)
O1	0.2078(4)	0.0370(2)	1.0834(4)	0.031(2)
O2	0.1056(6)	0.1687(3)	1.0841(6)	0.057(4)
O3	0.0362(7)	0.1431(3)	1.2727(7)	0.060(4)
O4	−0.0177(9)	−0.0331(4)	1.3347(7)	0.091(6)
O5	−0.0478(6)	−0.1008(3)	1.1523(6)	0.055(4)
O6	−0.0534(4)	−0.0030(3)	0.9733(4)	0.038(2)
O7	0.3403(4)	0.0143(2)	0.9218(4)	0.032(2)
O8	0.4893(9)	0.0675(4)	0.6528(7)	0.087(6)
O9	0.4418(6)	0.1265(3)	0.8223(6)	0.058(4)
O10	0.6120(7)	−0.1382(4)	0.9890(7)	0.071(5)
O11	0.5682(8)	−0.1103(3)	0.7628(7)	0.075(5)
O12	0.6079(4)	−0.0043(3)	1.0609(4)	0.046(3)
C1	0.1182(7)	0.0541(4)	1.1681(6)	0.035(4)
C2	0.0878(7)	0.1280(4)	1.1643(7)	0.041(4)
C3	−0.009(1)	0.2127(5)	1.281(1)	0.073(8)
C4	−0.019(2)	0.2255(7)	1.416(1)	0.14(2)
C6	−0.0315(6)	0.0154(4)	1.1111(6)	0.034(4)
C7	−0.0333(7)	−0.0427(4)	1.2116(8)	0.046(5)
C8	−0.045(1)	−0.1571(5)	1.246(1)	0.086(9)
C11	0.1187(8)	−0.1272(4)	0.9118(8)	0.045(5)
C12	−0.0306(9)	−0.1167(5)	0.830(1)	0.055(6)
C13	−0.0315(9)	−0.0963(5)	0.696(1)	0.064(6)
C14	0.116(1)	−0.0934(4)	0.6950(8)	0.055(6)
C15	0.2078(8)	−0.1148(4)	0.8281(8)	0.046(5)
C16	−0.0473(9)	0.1089(4)	0.7935(8)	0.049(5)
C17	0.0960(9)	0.1198(4)	0.7812(9)	0.053(5)
C18	0.1021(9)	0.0804(5)	0.6661(8)	0.057(6)
C19	−0.0311(9)	0.0469(5)	0.6102(7)	0.054(5)
C20	−0.1242(8)	0.0625(5)	0.6929(7)	0.050(5)
C21	0.4282(6)	0.0066(4)	0.8302(6)	0.037(4)
C22	0.4544(8)	0.0698(4)	0.7588(7)	0.045(5)
C26	0.5813(7)	−0.0217(4)	0.9194(7)	0.041(4)
C27	0.5883(8)	−0.0972(5)	0.9000(9)	0.053(5)
C28	0.567(1)	−0.1795(6)	0.724(1)	0.11(1)
C31	0.4373(8)	0.1338(4)	1.2771(8)	0.045(5)
C32	0.4528(9)	0.1494(5)	1.1418(8)	0.050(5)
C33	0.5939(8)	0.1295(4)	1.1448(8)	0.050(5)
C34	0.6642(8)	0.1005(5)	1.2774(7)	0.050(5)
C35	0.5700(8)	0.1063(4)	1.3599(8)	0.044(5)
C36	0.569(1)	−0.0425(5)	1.386(1)	0.062(6)
C37	0.5841(8)	−0.0826(5)	1.282(1)	0.057(6)
C38	0.4400(9)	−0.1025(4)	1.1998(9)	0.050(5)
C39	0.4193(9)	−0.0358(5)	1.3760(8)	0.050(5)
C40	0.3416(8)	−0.0741(4)	1.2595(8)	0.046(5)
C9	0.051(2)	−0.2091(9)	1.233(2)	0.078(5)
C9a	−0.043(3)	−0.212(1)	1.171(3)	0.077(7)
C23	0.451(1)	0.1924(7)	0.752(1)	0.099(4)
C24	0.586(3)	0.211(1)	0.782(2)	0.199(9)
C29	0.447(2)	−0.194(1)	0.603(2)	0.093(6)
C29a	0.532(3)	−0.189(2)	0.575(3)	0.085(8)

[a] $U_{eq} = \frac{1}{3} \sum_i \sum_j U_{ij} a_i^* a_j^* \mathbf{a}_i \cdot \mathbf{a}_j$.

moieties at the dimetallatricyclic dimer **2**. It is conceivable that the two zirconium–oxygen bonds (marked a in Scheme 3) which are connecting two monomeric

units are cleaved during the observed rearrangement process. Consequently, the equilibration process would then have to be described to proceed via monomeric $Cp_2\overline{ZrOCH(E)CH(E)O}$ intermediates and hence would constitute an intermolecular exchange process of mononuclear diethyltartratozirconocene moieties. Alternatively, the zirconium–oxygen bonds (marked b in Scheme 3) inside the five-membered rings of dimer **2** could be ruptured. The observed exchange process would then be strictly intramolecular in nature. The intra- and intermolecular pathways taken in a similar rearrangement of dimeric catecholatozirconocenes have recently been distinguished by means of a crossover experiment [6].

These two possible rearrangement pathways can very easily be distinguished by a simple cross-over experiment employing a mixture of the dimetallatricyclic ethyltartratozirconocene complex **2** with its enantiomer *ent*-**2**. A 1:1 mixture of the two enantiomers shows the same low temperature ^{1}H NMR spectrum (CD_2Cl_2, 225 K) as the optically pure complex **2**. However, at *c.* 270 K a second set of signals of the intermolecular crossover product, *meso*-**2**, is growing in. It exhibits signals at δ 6.27 and 6.21 (s, each 10H, Cp), 4.50 (s, 4H, C*H*(E)), 4.2 (m, 8H, CH_2) and 1.36 (t, 12H, CH_3). Equilibrium is reached after some time at 290 K at *rac*-**2**/*meso*-**2** $\approx$ 55:45. From the time dependence of this equilibration process starting from a *rac*-**2** enriched sample an activation barrier of $\Delta G^{\ddagger}_{inter}$ (290 K) of 22 ± 1 kcal mol^{-1} was derived. By the design of this specific experiment this constitutes the activation barrier of the intermolecular exchange process of mononuclear $Cp_2\overline{ZrOCH(E)CH(E)O}$ subunits. Therefore, we conclude that the faster equilibration process which is observed by dynamic ^{1}H NMR spectroscopy as described above must be due to a much more facile intramolecular pathway ($\Delta G^{\ddagger}_{intra}$ (265 K) $\approx 13 \pm 1$ kcal mol^{-1}) which could potentially proceed via a ten-membered dimetallamonocyclic intermediate (**3**) or transition state structure (Scheme 3).

The isomer *meso*-**2** shows a different behavior from the chiral dimetallatricyclus *rac*-**2**. Whereas the latter shows temperature dependent dynamic NMR spectra as described above, the ^{1}H NMR spectra of the *meso*-**2** complex do not change with temperature. Even at the lowest monitoring temperature (210 K, CD_2Cl_2 solution, 200 MHz) *meso*-**2** exhibits only one set of $-CH_2CH_3$ ^{1}H NMR signals and a single sharp singlet of the –C*H*(E)– ring methine protons. This means either that the intramolecular exchange process is proceeding at a much higher rate as compared to its diastereomer *rac*-**2** (and is thus not 'frozen' on the ^{1}H NMR time scale) or that the dimetallic tartratozirconocene complex *meso*-**2** is favoring a C_{2h}-symmetric ten-membered ring type structure (*meso*-**3**) in solution.

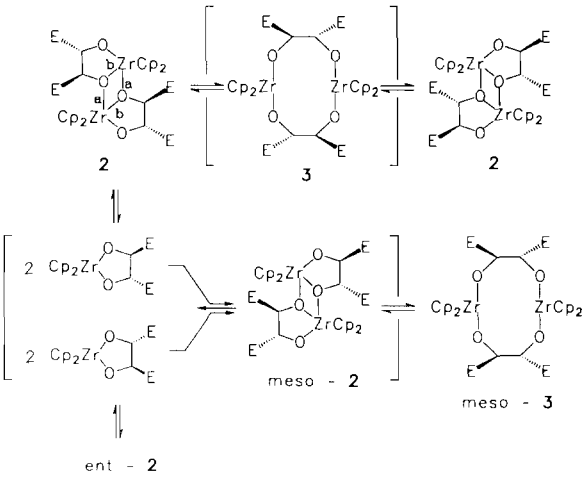

Scheme 3.

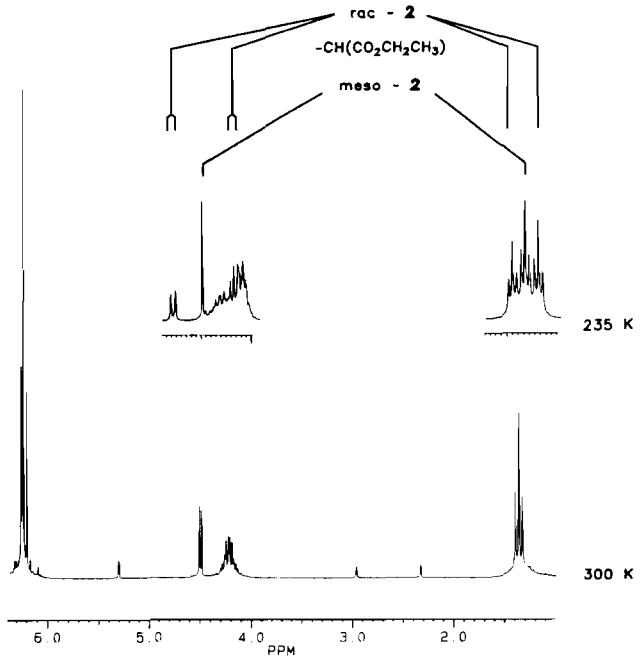

Fig. 2. ^{1}H NMR spectra (200 MHz in CD_2Cl_2) of a mixture of the complexes *meso*-**2** and *rac*-**2** at two temperatures.

^{1}H NMR spectra (200 MHz in CD_2Cl_2) of a mixture of the complexes *meso*-**2** and *rac*-**2** at two temperatures are given in Fig. 2.

Reaction of dimethylzirconocene with meso-dimethyltartrate

From the study described above it became evident that small stereochemical changes of the substituent pattern at the central framework of dimetallic tartratozirconocene complexes could induce drastic changes in the dynamic behavior or even possibly in their overall structural appearance. In order to investigate this remarkably strong structural response to rather subtle

alterations in stereochemical information at the perimeter of the metallacyclic framework we have prepared analogous (*meso*-tartrato)zirconocene complexes and looked at their structural properties in solution (by ^{1}H NMR spectroscopy) and in the solid state (by X-ray diffraction). We have reacted dimethylzirconocene **1** with one molar equivalent of *meso*-dimethyltartrate in methylene chloride solution at ambient temperature. Methane is evolved and the (*meso*-dimethyltartrato)-zirconocene complex **4** isolated in almost quantitative yield. The IR spectrum shows more than two strong ν(C=O) bands (1759, 1752, 1746 cm^{-1} with shoulders). The NMR spectra monitored at ambient temperature have revealed that two isomeric complexes are formed (**4a** and **4b** in a 60:40 ratio). Both products seem to be [$Cp_2ZrOCH(E)CH(E)O$] dimers. They are stereoisomers of different symmetry. Both products exhibit dynamic NMR spectra due to the presence of rearrangement processes being rapid on the NMR time scale. This has led to spectra monitored at the high temperature limiting situation pretending a higher molecular symmetry than is actually characteristic for the dinuclear complexes **4**.

The major product **4a** under these conditions exhibits the spectra of an apparently C_{2h}-symmetric species giving rise to the observation of ^{1}H NMR signals (CD_2Cl_2, 300 K, 200 MHz) at δ 6.26 (s, 20H, Cp), 4.87 (s, 4H, C*H*E) and 3.76 (s,m 12H, CH_3). (^{13}C NMR (CD_2Cl_2), 300 K, 50 MHz): δ 173.0 (CO), 112.0 (Cp), 85.5 (*C*HE), 51.8 (*C*H$_3$) (E=–CO_2CH_3).) The minor isomer **4b** has apparent C_{2v} symmetry and exhibits ^{1}H NMR signals under the same conditions at δ 6.28 and 6.23 (s, 10H each, Cp), 4.64 (s, 4H, C*H*E) and 3.74 (s, 12H, CH3). (^{13}C NMR: 173.0 (CO), 114.7 and 112.0 (Cp), 85.5 (C*H*E), 51.9 (*C*H$_3$).)

On lowering the monitoring temperature the ^{1}H NMR methyl singlet of complex **4b** is broadened and eventually splits into two singlets of equal intensity (CD_2Cl_2, 200 MHz, 230 K: δ 3.67 and 3.65). The –C*H*(E)– methine singlet separates into a well resolved AX pattern at δ 4.72 and 4.40 with a vicinal coupling constant of ^3J=5.1 Hz. We thus conclude that complex **4b** in solution has the typical dimetallatricyclic type structure (A-type in Scheme 1) and is undergoing a thermally induced rapid rearrangement process leading to symmetrization similarly to complex **2** as described above. From the ^{1}H NMR coalescence of the methyl singlets we have estimated a Gibbs-activation barrier for this process of complex **4b** a $\Delta G^{\ddagger}$ (285 K)$\approx$14$\pm$1 kcal mol^{-1}.

Similar dynamic ^{1}H NMR behavior is observed for complex **4a**. Here the methyl resonance splits into two equal-intensity singlets at δ 3.73 and 3.69 on lowering the temperature (CD_2Cl_2, 200 MHz, 220 K). At these conditions the –C*H*E– signal has split into two separate resonances (1:1 intensity) at δ 4.91 and 4.80. The activation energy of this rearrangement process of complex **4a** was determined from the methyl coalescence at $\Delta G^{\ddagger}$ (224 K)$\approx$11$\pm$1 kcal mol^{-1}. We conclude that the activation barriers for this process of the isomeric (*meso*-dimethyltartrato)zirconocene complexes **4a** and **4b** are both within the range typical for the intramolecular equilibration process of the dimetallatricyclic tartratozirconocene systems. Complexes **4a** and **4b** seem to favor this structural type in solution (see Scheme 4). The activation barrier of the slower intermolecular exchange (i.e. the **4a**$\rightarrow$**4b** rearrangement starting from a **4a** enriched sample) was determined at $\Delta G^{\ddagger}$ (300 K)=24.7$\pm$1.0 kcal mol^{-1}.

Crystallization from methylene chloride gave crystals suited for an X-ray crystal structure analysis. This X-ray diffraction study furnished a surprising result. The analyzed material, crystallized from a mixture of products **4a** and **4b** which clearly belonged to the dimetallatricyclic structural type **A** (see Scheme 1) in solution (as evidenced by the NMR analysis as described above), turned out to be a dinuclear (*meso*-dimethyltartrate)zirconocene dimer exhibiting a monocyclic ten-membered ring-type structure (type **B** in Scheme 1). The crystallized compound has the four ester substituents attached in a *cis,trans,cis*-manner at the ten-membered tetraoxadizirconacycle. In the crystalline state the dimetallatricyclic isomer **4a** seems to be less favorable than the monocyclic structural alternative **5a**.

Two views of the molecular structure of the (*meso*-dimethyltartrato)zirconocene dimer **5a** in the solid state are shown in Fig. 3. Selected bond lengths (Å) and angles (°) of **5a** are given in Table 3, and atomic coordinates in Table 4. Details of the X-ray crystal structure determinations of the tartratozirconocene complexes **2** and **5a** are presented in Table 5. See also 'Supplementary material'.

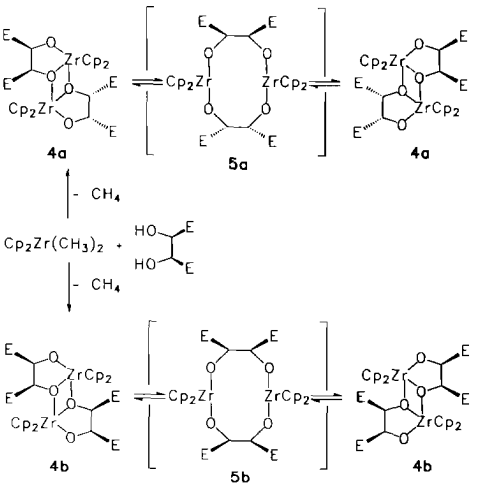

Scheme 4.

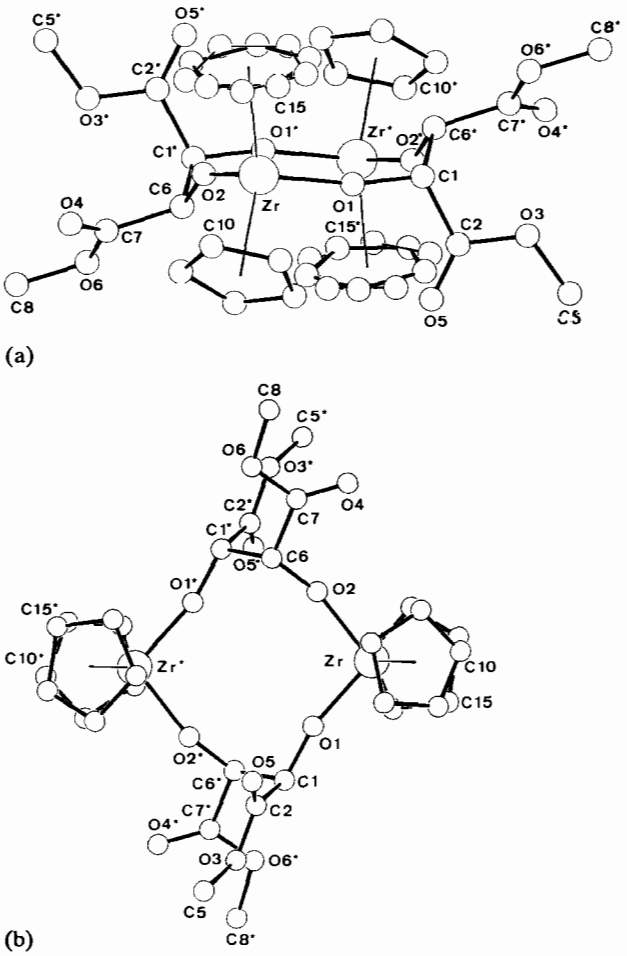

Fig. 3. Two views of the molecular structure of the (*meso*-dimethyltartrato)zirconocene dimer **5a** in the solid state (with unsystematical numbering scheme; two symmetry-related Cp rings are disordered).

TABLE 3. Selected bond distances (Å) and angles (°) of **5a**

Zr–O1	1.945(3)	Zr–O2	1.964(3)
O1–C1	1.371(5)	O2–C6	1.385(6)
C1–C6*	1.557(6)	C1–C2	1.515(7)
C6–C7	1.518(7)		
O2–Zr–O1	100.4(1)	C1–O1–Zr	163.0(3)
C6–O2–Zr	149.6(3)	C6*–C1–C2	107.7(4)
C6*–C1–O1	109.4(3)	C2–C1–O1	112.2(4)
C1*–C6–C7	112.6(4)	C1*–C6–O2	109.1(4)
C7–C6–O2	111.1(4)		

TABLE 4. Atomic coordinates and isotropic thermal parameters (Å^2) of **5a**

Atom	*x*	*y*	*z*	U_{eq}[a]
Zr	0.8558(1)	0.9343(1)	0.1103(1)	0.037(1)
O1	1.0267(3)	0.8969(2)	0.1215(3)	0.053(2)
O2	0.7964(3)	1.0246(2)	−0.0325(3)	0.056(2)
O3	1.3015(3)	0.7635(2)	0.1486(4)	0.074(3)
O4	0.5302(3)	1.0544(3)	−0.1970(4)	0.080(3)
O5	1.0899(4)	0.7619(3)	−0.0104(4)	0.075(3)
O6	0.5739(3)	1.0792(2)	−0.3644(3)	0.059(2)
C1	1.1582(4)	0.8714(3)	0.1683(4)	0.043(3)
C2	1.1748(5)	0.7942(3)	0.0888(5)	0.055(4)
C5	1.3390(6)	0.6940(5)	0.0823(7)	0.090(6)
C6	0.7587(4)	1.0448(3)	−0.1621(4)	0.047(3)
C7	0.6085(4)	1.0608(3)	−0.2387(5)	0.050(3)
C8	0.4354(6)	1.0987(4)	−0.4456(6)	0.077(4)
C10	0.6794(6)	0.8243(4)	0.1068(7)	0.081(6)
C11	0.7883(6)	0.7739(4)	0.1379(6)	0.076(5)
C12	0.8099(6)	0.7682(4)	0.0322(8)	0.080(6)
C13	0.7139(9)	0.8208(5)	−0.0651(6)	0.096(6)
C14	0.6302(5)	0.8575(4)	−0.0154(8)	0.087(5)
C15	0.920(1)	0.9481(6)	0.3497(9)	0.059(2)
C16	1.018(1)	0.9982(9)	0.333(1)	0.063(2)
C17	0.957(1)	1.0744(7)	0.254(1)	0.065(2)
C18	0.817(1)	1.0752(8)	0.218(1)	0.071(3)
C19	0.797(1)	1.0000(8)	0.279(1)	0.053(2)
C15a	0.989(2)	0.956(1)	0.358(2)	0.069(4)
C16a	1.000(1)	1.039(1)	0.306(1)	0.047(3)
C17a	0.885(2)	1.0854(9)	0.240(1)	0.057(3)
C18a	0.775(1)	1.035(1)	0.242(2)	0.060(3)
C19a	0.846(2)	0.961(1)	0.323(1)	0.056(3)

[a] $U_{eq} = \frac{1}{3}\sum_i \sum_j U_{ij} a_i^* a_j^* \mathbf{a}_i \cdot \mathbf{a}_j$.

Complex **5a** contains a ten-membered metallacyclic framework which has a chair-like arrangement of carbon, oxygen and zirconium atoms. In the crystal complex **5a** has C_i symmetry with atoms O2, Zr, O1, C1 and their symmetry related counterparts O2*, Zr*, O1* and C1* all located near a common central plane. Only carbon atoms C6 and C6* are located markedly outside this plane. They represent the 'tips' of the elongated chair-like framework of **5a**. The ester substituents are bonded to the carbon atoms C1, C6, C1* and C6*. Two of them (bonded to C6/C6*) are oriented pseudo-equatorially whereas the remaining $-CO_2CH_3$ groups at carbon centers C1/C1* are pointing away from the central framework towards pseudoaxial directions.

Each zirconium atom is bonded to the Cp ligands and to the two oxygen atoms which are directly adjacent. All other zirconium to oxygen separations are >4 Å and thus clearly outside of any bonding contact (e.g. the transannular separations are 4.27 (Zr–O1*) and 4.45 (Zr–O2*) Å; metal to carbonyl–oxygen distances are 4.12 (Zr–O4), 4.31 (Zr–O5) and 4.67 (Zr–O5*) Å).

It seems that the metallacyclic **B**-type structure (see Scheme 1) of complex **5a** is energetically favored in this situation primarily because it has allowed for the formation of four strong zirconium to oxygen bonds (including a substantial chalcogen to metal π-back-donating component). This is evident from the observed short zirconium–oxygen bond lengths at 1.945(3) (Zr–O1) and 1.964(3) (Zr–O2) Å [7] and further supported by the rather large O1–Zr–O2 angle of 100.4(1)° at the tetracoordinate zirconium center [1]. The bonding

TABLE 5. Details of the X-ray crystal structure determinations of the tartratozirconocene complexes **2** and **5a**

	2	**5a**
Formula	$C_{36}H_{44}O_{12}Zr_2$	$C_{32}H_{36}O_{12}Zr_2$
Molecular weight	851.2	795.1
Space group	$P2_1$ (No. 4)	$P2_1/c$ (No. 14)
a (Å)	9.494(1)	11.261(2)
b (Å)	20.122(2)	14.511(2)
c (Å)	9.915(1)	11.562(2)
β (°)	108.36(1)	117.81(1)
V (Å^3)	1797.7	1671.2
D_{calc} (g cm^{-3})	1.57	1.58
μ (cm^{-1})	6.29	6.71
Z	2	2
λ (Å)	0.71069	0.71069
Measured reflections	4445 ($\pm h$, $+k$, $+l$)	4149 ($\pm h$, $+k$, $+l$)
$[(\sin\theta)/\lambda]_{max}$ (Å^{-1})	0.65	0.65
Independent reflections	4202	3806
Observed reflections ($I > 2\sigma(I)$)	3811	3233
Refined parameters	439	203
R	0.039	0.047
R_w ($w = 1/\sigma^2(F_o)$)	0.046	0.063
Residual electron density (e Å^{-3})	0.58	0.56

angles at the ring-oxygen centers are 163.0(3)° (C1–O1–Zr) and 149.6(3)° (C6–O2–Zr). This large deviation towards sp-hybridized oxygen indicates that making very strong zirconium to oxygen interactions provides a sufficient energetic compensation to let the ten-membered monocyclic ring-structure (**5a**) of this dinuclear tartratozirconocene complex in the crystalline state successfully compete against the alternative dimetallatricyclic isomeric structure **4a**. However, these structural alternatives are probably rather close in energy since the latter seems to be favored in solution as judged from the NMR analysis discussed above.

Conclusions

From the chemistry related to Sharpless-oxidation catalysis it is well known that tartrato–Group 4 metal complexes exhibit a great structural diversity [8]. Many different types of polycyclic polynuclear tartratotitanium complexes have been isolated and structurally characterized. What is extraordinary about the tartratozirconocene complexes described here and in a related study [4] is the fact that two isomeric types, dimetallatricycle (**A**) and ten-membered monocycle (**B**), seem to be so close in energy that small changes at the molecule itself or in the surrounding environment are sufficient to make one or the other more favorable.

From the study of the dinuclear (*meso*-dimethyltartrato)zirconocene isomers **4** with a favored dimetallatricyclic structure in solution we have got some feeling for the magnitude of some of the energetic changes accompanied with alterations of the stereochemical placement of substituents at the metallacyclic perimeter. The observed isomers **4a** and **4b** both undergo an intramolecular automerization reaction which is probably proceeding via a ten-membered metallacyclic transition state or intermediate. We have measured the activation energies of this process for the separate isomers **4a** and **4b** and have found that they differ by about 3 kcal mol^{-1}. So it looks as if the *cis,trans,cis*-arrangement (as observed for **5a**) leads to a stabilization of the overall system by that amount as compared to the *cis,cis,cis*-alternative (**5b**). We do not see any strong effect by means of a direct interaction between the ester substituents at the metallacycle that may be causing such an energetic difference. It is rather likely that the metallacyclic ten-membered ring (in contrast to the isomeric dimetallatricyclic framework) is flexible enough to allow for the sterically best orientation of substituents attached to it. However, it appears that the overall ten-membered ring conformation is very much influenced by finding the best conformational positioning of the substituents at its rim. This can clearly be seen if the molecular structures of differently substituted tetraoxadimetallacyclodecane systems are compared [4]. The different ring conformations probably lead to substantial differences in the chalcogen to metal π-backbonding contribution of the four Zr–O units present. As these π-components seem to play a major role in the energetic compensation on going from the dimetallatricycle (**A**) to its ten-membered ring isomer (**B**) it is well conceivable that influencing the conformational properties of the medium-sized metallacyclic ring system by the substitution pattern as well as by external forces is a decisive factor for determining the favored molecular

structure of such tartrato–Group 4 transition metal compounds in a given situation.

This may create a potential difficulty if complexes of this general type are employed in catalytic processes (such as, for example, the (tartrato)$Ti(OR)_2$ dimers in Sharpless-oxidation catalysis) [9]. It may not be valid to draw direct conclusions between the structural properties of catalyst precursors and the structure of the alleged active catalyst itself. The necessary changes of substituents and attachment of reagents and products at the metal center may have caused major structural alterations of the metal complex framework similar to that observed for the catalytically inactive tartrato-zirconocene model systems described in this article. Therefore, we feel that any conclusions about the structural properties of such catalyst systems based on stoichiometric model systems should be supported by some additional experimental evidence providing, for example, a direct stereochemical information that is passed from the actual active catalyst onto an isolated catalytically formed reaction product [10].

Experimental

All reactions were carried out in an inert atmosphere (argon or nitrogen) using Schlenk-type glassware or in a glovebox. Solvents were dried and distilled under argon prior to use. The following spectrometers were used: Bruker AC 200 P NMR spectrometer (^1H, 200 MHz; ^{13}C, 50 MHz), Nicolet 5 DXC FT IR spectrometer. Melting points were determined by DSC (DuPont 2910 DSC, STA Instruments). Dimethylzirconocene was prepared according to a literature procedure [11].

Reaction of dimethylzirconocene with 2R,3R-diethyltartrate

Dimethylzirconocene **1** (3.5 g, 14.2 mmol) was dissolved in 80 ml of methylene chloride. To this solution was added dropwise 2.9 g (14.2 mmol) of 2*R*,3*R*-diethyltartrate at room temperature over a period of 0.5 h. The mixture was stirred for an additional hour. Then the solvent was removed *in vacuo*. The residue was washed with 5 ml of pentane and dried *in vacuo* to yield 6.0 g (98%) of **2**. The enantiomer *ent*-**2** was prepared analogously by reacting dimethylzirconocene with 2*S*,3*S*-diethyltartrate. The single crystals of complex **2** that were used for X-ray diffraction were obtained by crystallization from toluene. Details of the X-ray crystal structure analysis of **2** are given in Table 5. Characterization of complex **2**: m.p. = 77.0° (DSC). *Anal.* Calc. for $C_{36}H_{44}O_{12}Zr_2$ (851.2): C 50.80, H 5.21. Found C 50.91, H 5.26%. IR (KBr): ν(CO) = 1748, 1710 cm^{-1}. ^1H NMR (C_6D_6, 200 MHz, 300 K): δ 6.24 (s, 20H, Cp), 4.92 (s, 4H, CH), 4.08 (m, 8H, CH_2), 1.06 (t, 12H, CH_3). ^{13}C NMR ($CDCl_3$, 50 MHz, 300 K): δ 172.4 (CO), 112.4 (Cp), 84.4 (CH), 60.6 (OCH_2), 14.2 (CH_3).

Reaction of dimethylzirconocene with meso-dimethyltartrate

Dimethylzirconocene **1** (2.5 g, 10.0 mmol) was dissolved in 90 ml of methylene chloride. To this solution were added 1.8 g (10.0 mmol) of *meso*-dimethyltartrate in 15 portions during *c.* 0.5 h at room temperature. A vigorous gas evolution was observed (methane). The mixture was stirred for another hour at room temperature. Solvent was then removed *in vacuo* and the solid residue washed with 10 ml of pentane to yield 3.9 g (97%) of the (*meso*-dimethyltartrato)zirconocene dimer **4** (75:25 mixture of the *cis*- and *trans*-isomers **4a** and **4b**, as analyzed in solution; crystallization from methylene chloride furnished crystals of the isomer **5a** that were characterized by X-ray diffraction. For details concerning the X-ray crystal structure analysis of **5a** see Table 5.). Characterization of the **4a, 4b** mixture: m.p. = 50.0 °C (decomp., DSC). *Anal.* Calc. for $C_{32}H_{36}O_{12}Zr_2$ (795.1): C 48.34, H 4.56. Found C 47.96, H 4.62%. IR (KBr): ν(CO) = 1759, 1752, 1746 cm^{-1}. ^1H NMR (CD_2Cl_2, 200 MHz, 300 K), isomer **4a**: δ 6.26 (s, 20H, Cp), 4.87 (s, 4H, CH), 3.76 (s, 12H, OCH_3); isomer **4b**: δ 6.28 and 6.23 (s, each 10 H, Cp), 4.64 (br s, 4H, CH), 3.74 (s, 12H, OCH_3). ^{13}C NMR (CD_2Cl_2, 50 MHz, 300 K), isomer **4a**: 173.0 (CO), 112.0 (Cp), 85.5 (CH), 51.8 (OCH_3); isomer **4b**: δ 114.7 and 112.0 (Cp), 85.5 (CH), 51.9 (OCH_3), carbonyl carbon not positively identified, possibly identical with **4a**.

Supplementary material

Further details of the crystal structure investigations are available on request from the Fachinformationszentrum Karlsruhe, Gesellschaft für wissenschaftlich-technische Information mbH, D-7514 Eggenstein-Leopoldshafen 2, on quoting the depository number CSD 56176, the name of the authors, and the journal citation.

Acknowledgements

Financial support from the Fonds der Chemischen Industrie, the Alfried Krupp von Bohlen und Halbach-Stiftung, and the Minister für Wissenschaft und Forschung des Landes Nordrhein-Westfalen is gratefully acknowledged.

References

1 G. Erker, K. Engel, J. L. Atwood and W. E. Hunter, *Angew. Chem., 95* (1983) 506; *Angew Chem., Int. Ed. Engl., 22* (1983) 494; G. Erker, F. Sosna, R. Zwettler and C. Krüger, *Organometallics, 8* (1989) 450; G. Erker, F. Sosna, P. Betz, S. Werner and C. Krüger, *J. Am. Chem. Soc., 113* (1991) 564; D. W. Stephan, *Organometallics, 9* (1990) 2718; T. T. Nadisdi and D. W. Stephan, *Can. J. Chem., 69* (1991) 167.

2 H. Takaya, M. Yamakawa and K. Mashima, *J. Chem. Soc., Chem. Commun.,* (1983) 1283; K. Kropp, V. Skibbe, G. Erker and C. Krüger, *J. Am. Chem. Soc., 105* (1983) 3353; G. Erker, *Acc. Chem. Res., 17* (1984) 103; G. Erker, P. Czisch, R. Schlund, K. Angermund and C. Krüger, *Angew. Chem., 98* (1986) 356; *Angew. Chem., Int. Ed. Engl., 25* (1986) 364; G. Erker, U. Dorf, P. Czisch and J. L. Petersen, *Organometallics, 5* (1986) 668; G. Erker, U. Hoffmann, R. Zwettler, P. Betz and C. Krüger, *Angew. Chem., 101* (1989) 644; *Angew. Chem., Int. Ed. Engl., 28* (1989) 630.

3 J. C. Huffman, K. G. Moloy and K. G. Caulton, *Inorg. Chem., 27* (1988) 2190; B. Bachand and J. D. Wuest, *Organometallics, 10* (1991) 2015; R. B. Ortega, R. E. Tapscott and C. F. Campana, *Inorg. Chem., 21* (1982) 672.

4 G. Erker, S. Dehnicke, M. Rump, C. Krüger, S. Werner and M. Nolte, *Angew. Chem., 103* (1991) 1371; *Angew. Chem., Int. Ed. Engl., 30* (1991) 1349.

5 M. G. Finn and K. B. Sharpless, in J. D. Morrison (ed.), *Asymmetric Synthesis,* Vol. 5, Academic Press, New York, 1985, p. 247; K. B. Sharpless, S. S. Woodard and M. G. Finn, *Pure Appl. Chem., 55* (1983) 1823; M. G. Finn and K. B. Sharpless, *J. Am. Chem. Soc., 113* (1991) 113; P. G. Potvin, P. C. C. Kwong and M. A. Brook, *J. Chem. Soc., Chem. Commun.,* (1988) 773; P. G. Potvin, P. C. C. Kwong, R. Gau and S. Bianchet, *Can. J. Chem., 67* (1989) 1523.

6 G. Erker and R. Noe, *J. Chem. Soc., Dalton Trans.,* (1991) 685.

7 G. Erker, U. Dorf, C. Krüger and Y.-H. Tsay, *Organometallics, 6* (1987) 680, and refs. therein.

8 I. D. Williams, S. F. Pedersen, K. B. Sharpless and S. J. Lippard, *J. Am. Chem. Soc., 106* (1984) 6430; S. F. Pedersen, J. C. Dewan, R. R. Eckman and K. B. Sharpless, *J. Am. Chem. Soc., 109* (1987) 1279.

9 T. Katsuki and K. B. Sharpless, *J. Am. Chem. Soc., 102* (1980) 5974; S. S. Woodard, M. G. Finn and K. B. Sharpless, *J. Am. Chem. Soc., 113* (1991) 106; C. Puchot, O. Samuel, E. Dunach, S. Zhao, C. Agami and H. B. Kagan, *J. Am. Chem. Soc., 108* (1986) 2353; K. A. Jorgensen, R. Wheeler and R. Hoffmann, *J. Am. Chem. Soc., 109* (1987) 3240, and refs. therein.

10 E. J. Corey, *J. Org. Chem., 55* (1990) 1693; S. Tanako, Y. Iwabuchi and K. Ogasawara, *J. Am. Chem. Soc., 113* (1991) 2786; M. Hayashi, T. Matsuda and N. Oguni, *J. Chem. Soc., Chem. Commun.,* (1990) 1364.

11 P. C. Wailes, H. Weigold and A. P. Bell, *J. Organomet. Chem., 34* (1972) 155; E. Samuel and M. D. Rausch, *J. Am. Chem. Soc., 95* (1973) 6263.